Chemosphere 263 (2021) 127958

Contents lists available at ScienceDirect

Chemosphere

journal homepage: www.elsevier.com/locate/chemosphere

Quantifying the effect of nano-TiO_2 on the toxicity of lead on *C. dubia* using a two-compartment modeling approach

Xuesong Liu [a], Jianmin Wang [a, b, *], Yue-Wern Huang [b, c]

[a] Department of Civil, Architectural and Environmental Engineering, Missouri University of Science and Technology, Rolla, MO, 65409, United States
[b] The Center for Research in Energy and Environment (CREE), Missouri University of Science and Technology, Rolla, MO, 65409, United States
[c] Department of Biological Sciences, Missouri University of Science and Technology, Rolla, MO, 65409, United States

HIGHLIGHTS

- Nano-TiO_2 enhanced Pb body tissue accumulation in *C. dubia* through mouth ingestion.
- A two-compartment model was developed to quantify Pb body tissue accumulation.
- The Pb body tissue accumulation results in the toxicity of Pb.
- A toxicodynamic model could link Pb toxicity with the body tissue accumulation.
- Algae reduced Pb toxicity by reducing body tissue accumulation and the killing rate.

GRAPHICAL ABSTRACT

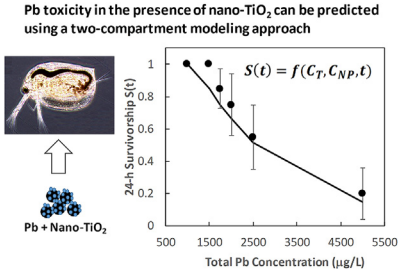

ARTICLE INFO

Article history:
Received 5 April 2020
Received in revised form
20 July 2020
Accepted 8 August 2020
Available online 15 August 2020

Handling Editor: Tamara S. Galloway

Keywords:
Nano-TiO_2
Lead
Toxicity
Algae
Two-compartment model
Toxicodynamic model

ABSTRACT

Nanoparticles (NPs) can significantly influence toxicity imposed by toxic metals. However, this impact has not been quantified. In this research, we investigated the effect of nano-TiO_2 on lead (Pb) accumulation and the resultant toxicity using water flea *Ceriodaphnia dubia* (*C. dubia*) as the testing organism. We used a two-compartment modeling approach, which included a two-compartment accumulation model and a toxicodynamic model, on the basis of Pb body tissue accumulation, to quantify the impact of nano-TiO_2 on Pb toxicity. The effect of algae on the combined toxicity of Pb and nano-TiO_2 was also quantified. The two-compartment accumulation model could well quantify Pb accumulation kinetics in two-compartments of *C. dubia*, the gut and the rest of the body tissue in the presence of nano-TiO_2. Modeling results suggested that the gut quickly accumulates Pb through active uptake from the mouth, but the rest of the body tissue slowly accumulates Pb from the gut. The predicted Pb distribution within *C. dubia* was verified by depuration modeling results from an independent depuration test. The survivorship of *C. dubia* as a function of Pb accumulated in the body tissue and exposure time can be well described using a toxicodynamic model. The effects of algae on Pb accumulation in different compartments of *C. dubia* and the toxicity in the presence of nano-TiO_2 were also well described using the two-compartment modeling approach. Therefore, the novel two-compartment modeling approach provides a useful tool for assessing the effect of NPs on aquatic ecosystems where toxic metals are present.

* Corresponding author. Department of Civil, Architectural and Environmental Engineering, Missouri University of Science and Technology, Rolla, MO, 65409, United States.
E-mail address: wangjia@mst.edu (J. Wang).

https://doi.org/10.1016/j.chemosphere.2020.127958
0045-6535/

1. Introduction

Recent anthropogenic activities have led to a significant release of nanoparticles (NPs) into the environment (Bundschuh et al., 2018). In addition to causing adverse environmental effects alone, NPs can also adsorb toxic metals and carry them into the body of aquatic organisms, enhancing the toxicity of the toxic metals. This effect challenges the existing toxicity evaluation paradigm for toxic metals (Fan et al., 2011; Hu et al., 2012a; Tan et al., 2011; Wang et al., 2011a, 2011b). Understanding the effects of NPs on the accumulation and distribution of toxic metals in aquatic organisms is essential in assessing metal toxicity in the presence of NPs.

Previous reports attributed NP-enhanced toxicity to an excessive accumulation of toxic metals in the whole body of the testing organism (Hu et al., 2012a, 2012b). For example, lead (Pb) accumulation in water flea *Ceriodaphnia dubia* (*C. dubia*) was increased by approximately 20 times in the presence of nano-TiO_2, leading to toxicity enhancement (Liu et al., 2019). In the absence of NPs, researchers have used a process-based kinetic modeling approach to quantify toxic metal accumulation in the entire body and the corresponding toxicity, based on the metal uptake, transfer, and depuration pathways (Cedergreen et al., 2017; Gao et al., 2016; He et al., 2019; Tan and Wang, 2012). However, because NPs alter the metal distribution pattern in different parts of the body, this whole body approach is unable to predict metal toxicity in the presence of NPs.

Gillis et al. (2005) proposed that the whole body of a *Daphnia* can be divided into two-compartments: the gut and the rest of the body tissue (referred as "tissue" hereafter). Heavy metals in the gut can be easily removed, thereby having less toxicity, but those in the tissue participate in the metabolic process and induce toxicity (Gillis et al., 2005; He et al., 2020). As a result, when assessing the effect of NPs on metal toxicity, models are needed to quantify metal accumulation in different compartments of *C. dubia*. Moreover, under realistic environmental conditions, other factors may also affect metal accumulation and distribution in the organism and, therefore, the toxicity (Fan et al., 2016; Tan et al., 2016). For example, algae inevitably impact heavy metal toxicity because they are extensively distributed as a natural food for aquatic organisms in the environment. Therefore, the effects of algae on metal bioavailability, distribution, and toxicity are also of great interest when assessing the metal toxicity in the presence of NPs.

A toxicodynamic model has been used to link toxic metal accumulation with toxicity (Cedergreen et al., 2017; Gao et al., 2016; He et al., 2019; Tan and Wang, 2012). The model describes a time-dependent hazard based on toxic metal accumulation in the entire body (Ashauer et al., 2010; Tan and Wang, 2012; He et al., 2020). However, because of the participation in the metabolic process and low elimination rate, heavy metals in the tissue are more relevant to toxicity than those in the gut (Gillis et al., 2005). NPs alter the metal distribution pattern within the body of an aquatic organism by disproportionally carrying significantly more toxic metals to the gut, toxicity prediction based on whole body accumulation is no longer appropriate. Metal distribution in different compartments of the aquatic organisms must be considered in the toxicodynamic model in order to better quantify the effect of NPs on metal toxicity.

In recent years, interactions between toxic metals and low toxic NPs have attracted significant attention (Hu et al., 2012a, 2012b; 2012c). Pb is one of the environmental hazards which has greatly raised public health concerns (Lewis, 1985). Nano-TiO_2 particles are considered low toxic and have been widely used in commercial products (Heinlaan et al., 2008). In this study, we developed a two-compartment accumulation model to predict the accumulation kinetics of Pb in the gut and the tissue of *C. dubia* in the presence of nano-TiO_2. The Pb accumulated in the tissue was applied to the toxicodynamic model to predict toxicity. We used *C. dubia*, an EPA recommended toxicity test organism, as the indicator organism for toxicity (EPA, 2002). We also quantified the effect of *Raphidocelis*, a common freshwater algae, on Pb accumulation and toxicity in the presence of nano-TiO_2, to shed light on the impact of naturally occurring algae on the combined toxicity of Pb and NPs.

2. Theoretical aspects

2.1. Two-compartment accumulation model

Toxic metals can accumulate in both the gut and the tissue, with each compartment having independent uptake pathways. The toxic metal accumulated in the gut is from active uptake through the mouth, and that accumulated in the tissue is in part from the surrounding environment through diffusion (Wang et al., 2014). In addition, the gut, as the digestive system, is responsible for nutrient transport via both passive and active mechanisms (Kiela and Ghishan, 2016). Therefore, toxic metals in the gut can also transfer into the tissue. The gut and the tissue also have independent pathways to depurate toxic metals from *C. dubia* (Gillis et al., 2005). Fig. 1 schematically illustrates the two-compartment model of uptake, depuration, and transfer of toxic metals in *C. dubia*. We propose the mathematical equations below to delineate the accumulation kinetics of toxic metals:

$$C_T(t) = C_{gut}(t) + C_{tissue}(t) \quad (1)$$

$$\frac{dC_{gut}(t)}{dt} = k_{in} - (k_{12} + k_{1e}) \times C_{gut}(t) \quad (2)$$

$$\frac{dC_{tissue}(t)}{dt} = jC_D(t) + k_{12}C_{gut}(t) - k_{2e}C_{tissue}(t) \quad (3)$$

where $C_T(t)$ = total toxic metal accumulated in the whole body (ng/flea) at time t; $C_{gut}(t)$ = toxic metal accumulated in the gut (ng/flea) at time t; $C_{tissue}(t)$ = toxic metal accumulated in the issue (ng/flea)

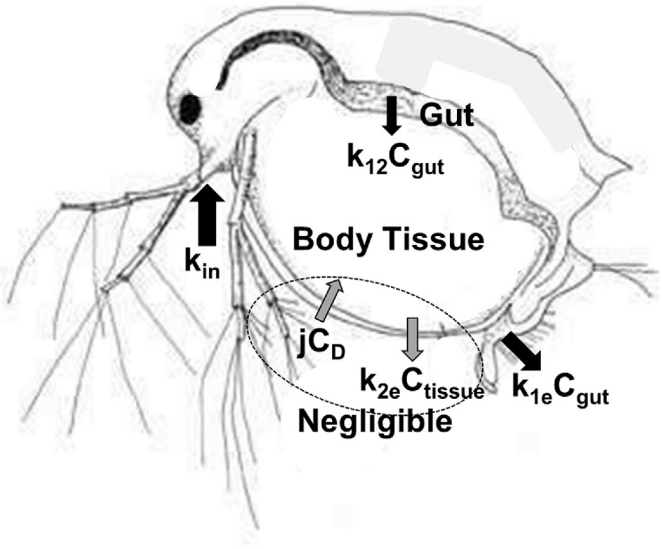

Fig. 1. Schematic of a two-compartment accumulation model. Gut accumulation considers active uptake through the mouth (k_{in}), losses to body tissue ($k_{12}C_{gut}(t)$), and losses to the outside ($k_{1e}C_{gut}(t)$). Body tissue accumulation considers influx from the outside ($jC_D(t)$) and influx from the gut ($k_{12}C_{gut}(t)$), as well as losses to the outside ($k_{2e}C_{tissue}(t)$). The Pb exchange between the body tissue and the surrounding solution through diffusion is negligible.

at time t; $C_D(t)$ = dissolved toxic metal concentration (ng/L) at time t; k_{in} = toxic metal gut influx rate (ng/flea/h); k_{12} = toxic metal transfer rate constant from the gut to the tissue (h^{-1}); k_{1e} = toxic metal depuration rate constant from the gut (h^{-1}); j = the tissue accumulation rate constant that reflects the diffusion from the surrounding solution to the tissue (L/flea/h); k_{2e} = tissue depuration rate constant that reflects the diffusion from the tissue to the surrounding solution (h^{-1}); t = exposure time (h).

Toxic metals in water are either associated with particles or in a soluble form. The particulate forms of toxic metals, including the metal precipitates and metals adsorbed by NPs, are accumulated in the gut through active uptake by *C. dubia*. Settled particles can also be re-suspended and ingested by *C. dubia* (Horton et al., 1979). Here we assume that the gut uptake rate of Pb is proportional to the adsorbed Pb concentration on the NP surface. In a system that contains Pb and nano-TiO_2, nearly 100% of Pb is adsorbed by nano-TiO_2 (Liu et al., 2019). Thus, we used the total Pb concentration to calculate the adsorbed Pb concentration by nano-TiO_2. Therefore, the influx rate of Pb to the gut through active ingestion from the mouth, in the presence of NPs, can be expressed as:

$$k_{in} = \frac{C_T}{C_{NP}} \times k \tag{4}$$

where C_T = total toxic metal concentration (ng/L); C_{NP} = the NP concentration (mg/L); k = the gut uptake constant through active mouth uptake (mg/flea/h).

The above differential equations were solved by using the WolframAlpha to find the analytical solution, which was used to conduct data fitting and find the related Pb accumulation kinetic constants (WolframAlpha, 2009). As a result, the metal accumulation in different compartments in the presence of NPs, e.g., the effect of NPs on metal distribution, can be calculated using the kinetic constants.

2.2. Two-compartment depuration model

A two-compartment depuration kinetic model was used to fit the experimental data from an independent depuration test, and to determine the metal distribution at the beginning and during the depuration process (Gillis et al., 2005). Results from this depuration model were used to validate the metal distribution from the accumulation model. The depuration model assumes that depurations, from both the gut and the tissue, follow first-order kinetics:

$$M_T(t) = M_{gut}(0)e^{(-k_g t)} + M_{tissue}(0)e^{(-k_t t)} \tag{5}$$

where $M_T(t)$ = mass of heavy metal in the whole body (ng/flea) at time t during depuration; $M_{gut}(0)$ = mass of heavy metal in the gut at the beginning of depuration (ng/flea); $M_{tissue}(0)$ = mass of heavy metal in the tissue at the beginning of depuration (ng/flea); k_g = the gut depuration rate constant (h^{-1}); k_t = the body depuration rate constant (h^{-1}); t = the depuration time (h). Note that $M_{gut}(0)$ and $M_{tissue}(0)$ in the depuration equation are equal to $C_{gut}(t)$ and $C_{tissue}(t)$ for the accumulation equation, where t is the time used to accumulate Pb before depuration tests.

The kinetic parameters were determined by using the least-squares algorithm during the nonlinear regression analysis of the experimental data. The quality of the data fitting was evaluated by the coefficient of determination (R^2).

2.3. Toxicodynamic model

A toxicodynamic model can be used to predict toxicity in terms of survivorship, based on the metal accumulation data calculated from the two-compartment accumulation model. The principle of this toxicodynamic model is that, if toxic metal accumulation in the tissue (metabolically available) exceeds a threshold value, hazard starts to accumulate, resulting in an increase in the probability of death (Cedergreen et al., 2017; Gao et al., 2016; Tan and Wang, 2012). Conventionally, the hazard development rate was defined in proportion to the toxic metal concentration that was in excess of the threshold level (Tan and Wang, 2012). For this research, we modified the hazard definition, and hypothesized that the maximum exceedance of the toxic metal tissue accumulation contributes equally with exposure time to the hazard. This hypothesis is similar to the C*t (disinfectant concentration × time) concept used for water disinfection process – a certain C*t value is correlated to a certain level of disinfection. Because the Pb tissue accumulation increases with an increase in the exposure time, the terminal Pb tissue accumulation at the end of the exposure, $C_{tissue}(t)$, is the maximal Pb tissue accumulation. As a result, the hazard can be expressed as:

$$H(t) = k_k \times (C_{tissue}(t) - C_{TH})t \tag{6}$$

where H(t) = hazard (dimensionless) at time t; k_k = killing rate (flea/ng/h); C_{TH} = toxic metal threshold concentration (ng/flea).

For this research, the negative control group did not show any toxicity. Therefore, the survival probability can be expressed as (Tan and Wang, 2012):

$$S(t) = \begin{cases} 1 & if\ C_{tissue}(t) \le C_{TH} \\ e^{-H(t)} & if\ C_{tissue}(t) > C_{TH} \end{cases} \tag{7}$$

where S(t) = survival probability of the test organism at time t.

By combining Equations (6) and (7), we obtain a modified toxicodynamic model for this application:

$$S(t) = \begin{cases} 1 & if\ C_{tissue}(t) \le C_{TH} \\ e^{-k_k \times (C_{tissue}(t) - C_{TH})t} & if\ C_{tissue}(t) > C_{TH} \end{cases} \tag{8}$$

Kinetic parameters were determined by using the least-squares algorithm during the nonlinear regression analysis of the experimental data. The quality of the data fitting was evaluated by the coefficient of determination (R^2).

3. Materials and methods

3.1. Chemicals, NPs, organisms, and solutions

All the chemicals used in this research were acquired from Fisher Scientific (Fair Lawn, New Jersey, USA), unless otherwise specified. $CaSO_4 \cdot 2H_2O$ (98%), Na_2SeO_4 (99%), $NaHCO_3$ (100.2%, Pb < 5 mg/kg), $MgSO_4$ (Pb < 0.001%), and KCl (99%) were used to prepare a culture medium buffer (Supplementary information). $Pb(NO_3)_2$ was used to prepare the Pb stock solution. Trace metal grade nitric acid was used for sample digestion. A certified Pb standard solution, at 1000 mg/L, was used to develop standard calibration curves for Pb analyses. Nano-TiO_2 (5–10 nm, anatase, 99%), purchased from Skyspring Nanomaterials Inc. (Houston, TX, USA), was used to prepare testing solutions. Algae (*Raphidocelis*) and a mixture of yeast, trout chow, and cereal leaves (YTC) (Pb < 1 μg/L), acquired from ABS Inc. (Fort Collins, CO, USA), were used as daily food for the *C. dubia* mass culture. The same algae (*Raphidocelis*) were also used in the accumulation, depuration, and toxicity tests. The starter *C. dubia* was purchased from MBL Aquaculture (Sarasota, FL, USA), and cultured in our lab using a culture medium that contained 1.8×10^5 cell/mL of algae and 6.8 mg/L of YTC (as a total solid), based on the EPA standard method, EPA-821-R-02-012 (EPA, 2002).

All test solutions were prepared using Milli-Q (MQ) water (resistivity = 18.2 MΩ cm). The culture medium buffer, moderate hardness synthetic water (pH = 7.8 ± 0.2, hardness = 85 ± 5 mg/L as $CaCO_3$), was prepared by dissolving appropriate amounts of $CaSO_4 \cdot 2H_2O$, Na_2SeO_4, $NaHCO_3$, $MgSO_4$, and KCl into MQ water, following the EPA standard method (EPA, 2002). The stock solution of 1000 mg/L Pb(II) was prepared by dissolving an appropriate amount of $Pb(NO_3)_2$ in MQ water, and then acidified it with trace metal grade nitric acid to a pH of less than 4 to prevent Pb precipitation.

All mass culture and toxicity tests were conducted in a laminar flow hood (SVC-6AX, Streamline® laboratory products, Fort Myers, FL, USA) within a temperature-controlled chamber (25 °C). The chamber was set at a light to dark cycle of 16 h–8 h to mimic the natural day and night light cycle.

3.2. Accumulation test

C. dubia neonates were used to conduct Pb toxicity tests according to EPA procedures (EPA, 2002). Ideally, the same *C. dubia* neonates should be used to conduct Pb accumulation and depuration tests. However, because the neonates were extremely fragile and could not survive the multiple manual steps of the accumulation and depuration tests, it was not practical to use them for both of these tests. Instead, we used *C. dubia* adults (2 weeks old) to conduct the Pb accumulation and depuration tests, and used this information to elucidate the Pb accumulation pattern in neonates.

In order to evaluate the toxicity in the acute test, relatively high concentrations of Pb and nano-TiO_2 were used in the accumulation and toxicity tests. For the accumulation test, a test solution containing 2500 μg/L of Pb(II) was prepared by diluting the Pb stock solution with 1 L of culture medium buffer in a 1 L HDPE bottle. A total of 50 mg of dry nano-TiO_2 particles was also added to the bottle to obtain a 50 mg/L nano-TiO_2 concentration. The test solution was then mixed using a mechanical shaker for 24 h. After mixing, approximate 10 mL of the test solution was collected to test the final pH, which was determined to be in the range of 7.4–7.8. This test solution was then used to conduct an accumulation test using a series of 125 mL HDPE bottle reactors that contained 100 mL of the test solution each.

Adult *C. dubia* (2 weeks old) were used to conduct the accumulation test. Four reactors, representing four accumulation time points, 1, 2, 4, and 6 h, respectively, were used. For each reactor, approximately 50 adult *C. dubia* were used. Before being added to the reactor, the *C. dubia* were washed three times with a clean culture medium buffer to eliminate any food adsorbed on the surface of the *C. dubia* during culturing. The *C. dubia* were then placed in the reactor for an accumulation test. After designated exposure time periods (1, 2, 4, or 6 h), the *C. dubia* were collected and washed three times with the clean culture medium buffer to remove particles from the surface. The *C. dubia* were then filtered through a 0.297 mm sieve, counted, and transferred to a digestion vessel that contained 5 mL of nitric acid. They were digested at 95 °C for 12 h in a hotblock digester with a Watlow mini controller (Watlow mini-0R10-000G). The digested sample was then diluted and analyzed for soluble Pb analysis. The total Pb content in each *C. dubia* was then calculated, based on the soluble Pb concentration of the digestion solution. A control group that did not contact the test solution was also digested and used to determine the background Pb content, which was 0.12 ng/flea. The net accumulation of Pb during the accumulation process was calculated by subtracting the background Pb content from the total Pb content. All accumulation experiments were conducted in duplicate.

The impact of algae on Pb accumulation was also tested by following a similar procedure as above, except that the test solution contained not only 2500 μg/L of Pb and 50 mg/L of nano-TiO_2, but also algae. Two algae concentrations, 1.8×10^5 and 5.4×10^5 cell/mL, respectively, were used. The algae concentrations were achieved by transferring appropriate volumes of the algae stock solution (3×10^7 cell/mL) to a test solution containing Pb and nano-TiO_2.

3.3. Depuration test

The Pb depuration test was conducted by following the procedure used by Gillis et al. (2005). In brief, six groups of *C. dubia,* representing six depuration times, 0, 1, 2, 4, 6, and 8 h, were used for the test. Each group contained approximately 50 adult *C. dubia*. Before depuration, each group *C. dubia* was placed in a 100 mL test solution that contained 2500 μg/L of Pb and 50 mg/L of nano-TiO_2 for 2 h, respectively, to uptake Pb. The *C. dubia* were then collected and washed three times with a clean culture medium buffer to remove any residual Pb from the surface. The group of *C. dubia* with a 0 h depuration time was directly digested without going through the depuration process. The rest of the five groups of *C. dubia* were transferred to five reactors that contained 100 mL of depuration solution (clean culture medium buffer + 1.8×10^5 cell/mL of algae), respectively, for depuration. After pre-selected depuration times (1, 2, 4, 6, and 8 h), *C. dubia* were collected, washed, filtered, counted, and digested in nitric acid. The Pb concertation in the digestion solution was measured and used to calculate the total Pb content in the *C. dubia*. The background Pb content was determined by using a group of 50 *C. dubia* that did not go through the Pb uptake and depuration procedures and was the same as that measured for the accumulation control group (0.12 ng/flea). The final accumulated Pb in *C. dubia* was calculated by subtracting the background Pb content from the total Pb content.

3.4. Toxicity test

The toxicity tests were conducted by following an EPA method (EPA, 2002). Two types of toxicity tests were conducted. The first type was to determine the effect of exposure time on toxicity and the second type was to determine the effect of Pb concentration on 24 h toxicity.

For the first type of toxicity test (effect of exposure time), two test solutions were used: both contained 2500 μg/L of Pb and 50 mg/L of nano-TiO_2, while one was supplemented with 1.8×10^5 cell/mL of algae. For each test solution, the survivorship of *C. dubia* neonates in different exposure times (ranging from 0 to 24 h) were monitored each hour. In brief, a total of 20 healthy neonates (at an age of less than 24 h) and four 30 mL medicine cup reactors (containing 15 mL of the test solution each) were used. Five neonates were washed three times with the clean culture medium buffer to remove residual food from their surface before transferring them to each test reactor. A plastic dropper, with a 3 mm diameter opening, was used to transfer neonates to prevent any damage to them. The survival of the neonates was visually monitored each hour, and dead neonates were removed from the test reactor until 24 h had elapsed.

For the second type of test (effect of Pb concentration), two series of test solutions were used: both contained Pb in a series of different concentrations (1,000, 1,500, 1,750, 2,000, 2,500, and 5000 μg/L) and the same 50 mg/L of nano-TiO_2, and one was supplemented with 1.8×10^5 cell/mL of algae. Procedures were the same as that described above for the first type of toxicity test, except that four replicate reactors were used for each Pb concentration and survival was examined only after 24 h of exposure. Different Pb concentrations were used to validate the toxicodynamic model parameters determined from the first type of toxicity

test (effect of exposure time).

3.5. Analytical method

To determine the soluble Pb concentration in test solutions, 10 mL of the solution was first centrifuged at 2000 G for 10 min to remove particles. The supernatant was then collected, acidified, and analyzed using a graphite furnace atomic absorption spectrophotometer (GFAA) (Perking Elmer AAnalyst 600), which has a Pb detection limit of 0.5 μg/L. The Pb concentration results and instrument performance were checked periodically by using certified Pb standard solution. The acceptance range of sample recovery and instrument performance were set to be 80–120% and 90–110% of certified Pb standard solution, respectively.

4. Results and discussion

4.1. Pb accumulation in the presence of nano-TiO_2

Fig. 2 shows the Pb accumulation data (filled circles) in *C. dubia* during the 6 h testing period. Equations (1)–(3) were used to fit the experimental data. The modeling result (solid line) was in good agreement with the experimental data (R^2 = 0.98). The related model parameters were also determined, shown in Table 1. By using the model parameters, we were able to estimate the Pb accumulation in different compartments of *C. dubia*. The dashed line was the estimated gut accumulation of Pb. The estimation indicates that gut Pb accumulation was very fast and took less than 2 h to reach the maximum value. The fast gut accumulation was caused by the active uptake of the particulate Pb through the mouth. The dotted line in Fig. 2 shows the modeled Pb tissue accumulation, which gradually increased at a relatively constant rate. Compared to gut accumulation, Pb tissue accumulation was much slower. Pb is a non-essential element, which does not have any physiological function in cells or specific uptake pathways (ICMM, 2007). In addition, Pb uptake has been shown to be mainly through the calcium (Ca) ion channel (Kerper and Hinkle, 1997). Our culture medium was a moderately hard water, which had a much higher Ca concentration than Pb. These resulted in a slow Pb tissue accumulation.

We also used Equations (1)–(3) to model the accumulation of iron (Fe), an essential element, using a test solution that contained 2500 μg/L of Fe and 50 mg/L of nano-TiO_2 (Fig. S1, supplementary information). The purpose of this test was to determine the difference between non-essential elements and essential elements in terms of tissue accumulation. Experimental data showed that Fe had an accumulation pattern that was similar to that of Pb. However, Fe exhibited a significantly higher tissue accumulation rate than Pb. This was because Fe is an important component in the electron transport chain during the metabolic process (Wang and Pantopoulos, 2011).

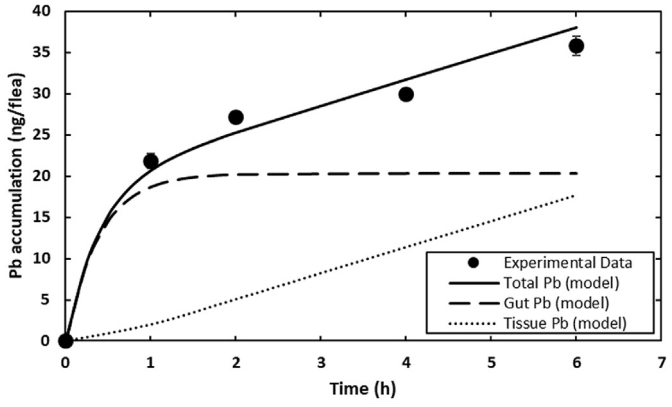

Fig. 2. Accumulation of Pb in *C. dubia* in the presence of nano-TiO_2. Condition of the exposure medium: [Pb] = 2500 μg/L; [nano-TiO_2] = 50 mg/L.

4.2. Model simplification

Table 1 shows that the tissue accumulation rate constant j, that denotes Pb diffusion from the surrounding test solution to the tissue, was very small. In addition, the body depuration rate constant k_{2e}, that indicates Pb depuration from tissue to surrounding solution through diffusion, was also very small, much smaller than the constant gut depuration rate constant k_{1e}. Therefore, the tissue had very little ability to directly accumulate Pb from and depurate Pb to the surrounding solution. Consequently, we could simplify the tissue accumulation kinetic model by neglecting these two pathways:

$$\frac{dC_{tissue}(t)}{dt} = k_{12}C_{gut}(t) \tag{9}$$

The corresponding analytical solutions for the simplified version of the two-compartment accumulation model (Equations (1), (2), and (9)) are:

$$C_{gut}(t) = \frac{\frac{C_T}{C_{NP}} \times k}{k_{12} + k_{1e}} \times \left(1 - e^{-(k_{12}+k_{1e})t}\right) \tag{10}$$

$$C_{body}(t) = \frac{\frac{C_T}{C_{NP}} \times k \times k_{12} e^{-(k_{12}+k_{1e})t}\left(e^{(k_{12}+k_{1e})t} \times (k_{12}t + k_{1e}t - 1) + 1\right)}{(k_{12}+k_{1e})^2} \tag{11}$$

The curve fitting results and related constants, using Equations (10) and (11), are also presented in Fig. 2 and Table 1. Note that the new curve from the simplified model completely overlaps with the curve that is based on the original model. Importantly, the new constants are also consistent with the ones obtained before simplification. Modeling results revealed that active ingestion through the mouth was the only meaningful Pb accumulation pathway, not only for the gut, but also for the tissue of *C. dubia*. In addition, all Pb depuration occurred from the gut.

The direct tissue accumulation of Pb from a solution could be through a slow diffusion process such as that of arsenic (Wang et al., 2014). In addition, in the presence of nano-TiO_2, the soluble Pb concentration was reduced to a very low level (<10 μg/L) due to adsorption of Pb by nano-TiO_2, which further reduced the driving force for diffusion. Therefore, the direct accumulation of Pb from solution was negligible, as compared to that from the active mouth uptake and gut transfer. The direct tissue depuration of heavy metals to the surrounding solution was an ATP-based biological process, which involved specific transporters (Silver, 1996). This resulted in a very low Pb depuration rate, which was negligible when compared to that from the gut depuration. This is supported by Gillis et al. (2005) who also reported very low heavy metal depuration rates from the tissue of *D. magna*. On the contrary, the heavy metal depuration from the gut was influenced by gut pH, which was 6.0–6.8 for *C. dubia* (Ebert, 2005). Pb carried into the gut by the nano-TiO_2 could be desorbed within the gut and quickly flushed out of *C. dubia* through the anus. Furthermore, the newly ingested nano-TiO_2 could then physically squeeze the previously accumulated nano-TiO_2, along with the adsorbed Pb, out of the gut

Table 1
Two-compartment accumulation model parameters.

Test Solution[a]	k (mg/flea/h)	j (L/flea/h)	k_{12} (h^{-1})	k_{1e} (h^{-1})	k_{2e} (h^{-1})	AE[b] (%)	R^2
Before model simplification							
Pb + nano-TiO_2	1.022×10^{-3}	1×10^{-6}	0.155	2.357	1×10^{-3}	6.175	0.98
After model simplification							
Pb + nano-TiO_2	1.022×10^{-3}	N.A.	0.155	2.357	N.A.	6.175	0.98
Pb + nano-TiO_2+algae (1.8×10^5 cell/mL)	0.926×10^{-3}		0.080	2.357		3.282	0.93
Pb + nano-TiO_2+algae (5.4×10^5 cell/mL)	0.693×10^{-3}		0.080	2.357		3.282	0.95

[a] All test solutions contain [Pb] = 2500 μg/L; [nano-TiO_2] = 50 mg/L.

[b] AE = assimilation efficiency; $AE = \frac{k_{12}}{k_{12}+k_{1e}}$ (Pan et al., 2016).

through the anus (Gillis et al., 2005). Both processes led to a much greater Pb depuration rate from the gut than that from the tissue.

4.3. Depuration modeling

We conducted a depuration experiment in a test solution that contained 1.8×10^5 cell/mL of algae. The algae was used to support the life of *C. dubia* and also speed up the depuration process. The depuration data were modeled using Equation (5) to determine the depuration kinetic constants. These constants were then used to calculate the Pb distribution in the *C. dubia* compartments at different depuration times, including at the beginning of the depuration. For this experiment, the *C. dubia* were initially exposed to a test solution that contained 2500 μg/L of Pb and 50 mg/L of nano-TiO_2 for 2 h, to accumulate Pb before placing them into the depuration solution. Therefore, the Pb accumulation in both compartments after 2 h of exposure in this test solution could also be determined using the depuration model. Fig. 3 shows the experimental Pb depuration results (filled circles), model calculations (smooth curves), and model parameters. Results suggest that the depuration was mostly from the gut (dashed line), and that there was hardly any depuration from the tissue (dotted line). The high depuration rate from the gut was most likely caused by the algae, which can quickly remove nano-TiO_2 along with adsorbed Pb from the gut. After 8 h of depuration, all Pb in the gut was eliminated. In contrast, tissue depuration of Pb is an biological process that needs a specific transporter (Silver, 1996), which was extremely slow. Therefore, the reduced Pb content during the depuration process was from gut elimination, and the remaining Pb after depuration was mostly in the tissue. The depuration modeling results indicated that, at the beginning of the depuration process (i.e., after 2 h of exposure in a test solution containing 2500 μg/L of Pb and 50 mg/L of nano-TiO_2), Pb accumulation in the gut and in the tissue were 22 ng/flea and 5.2 ng/flea, respectively. These results are in good agreement with those from the accumulation modeling when using Equations (10) and (11), which showed 20.2 ng/flea in the gut and 5.2 ng/flea in the tissue. This confirms that the two-compartment accumulation model is appropriate to quantify Pb accumulation in each compartment of the *C. dubia*.

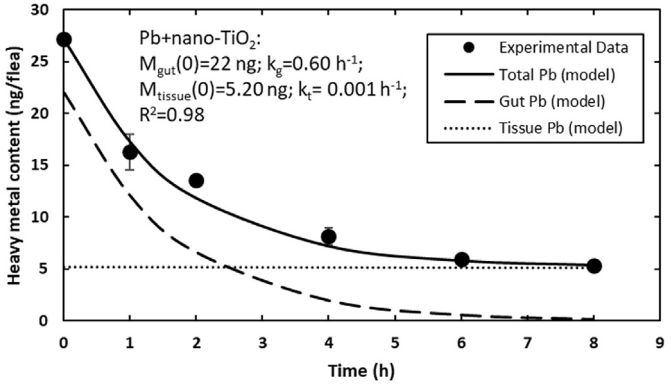

Fig. 3. Pb depuration from *C. dubia* in a culture medium that contained algae (1.8×10^5 cell/mL) after exposure in a medium that contained Pb and NPs. Conditions of the exposure medium: [Pb] = 2500 μg/L; [nano-TiO_2] = 50 mg/L; pre-exposure time before depuration: 2 h.

As indicated in Fig. 3, the Pb in the gut was completely depurated in 8 h. However, the Pb in the tissue did not change in the 8 h depuration period. Therefore, the Pb accumulation in the entire body after 8 h of depuration can be considered as the Pb in the tissue throughout the entire depuration period, including the beginning of the depuration process. The Pb accumulation in the gut at the beginning of depuration can be estimated by subtracting the Pb accumulation in the tissue (i.e., the Pb in the entire body after 8 h of depuration) from the total Pb accumulation in the entire body at the beginning of depuration. Therefore, by measuring the Pb in the entire body of *C. dubia* at the beginning of depuration and after 8 h of depuration, respectively, we could estimate the Pb accumulation in the gut and that in the tissue at the beginning of depuration.

4.4. Algae impact on Pb accumulation

The widely distributed algae are a natural food source for aquatic organisms. Therefore, when investigating the toxicity of contaminants, the effect of algae should be considered. Many studies have shown that algae can enhance the accumulation of toxic metals and/or NPs in organisms and, therefore, affect their toxicity (Liu et al., 2019; Petersen et al., 2009; Su et al., 2018; Svensson, 2003). Fig. 4 shows Pb accumulation data (filled circles) in the presence of 2500 μg/L of Pb and 50 mg/L of nano-TiO_2 under two algae concentrations, 1.8×10^5 cell/mL and 5.4×10^5 cell/mL, respectively. By fitting the experimental data using the simplified two-compartment accumulation model, Equations (10) and (11), we could determine the accumulation kinetic constants as effects of algae, shown in Table 1. These constants were used to calculate Pb accumulations in the gut and the tissue (shown as dashed and dotted curves, respectively).

The Pb accumulation pattern was similar to that without algae. However, algae reduced Pb accumulation in both the gut and the tissue. We also validated the two-compartment accumulation model by using depuration experimental results (data not shown). The model parameters in Table 1 suggest that the presence of algae significantly reduced the gut uptake constant k of Pb. Because algae had a much lower Pb adsorption capacity than nano-TiO_2 (Liu et al., 2019), and they occupied some gut space after ingestion, the accumulation of nano-TiO_2 and associated Pb was reduced in *C. dubia*. The small insert in Fig. 4b shows that the Pb gut uptake of rate constant k was linearly reduced with an increase in algae concentration. The model parameters also indicate that, for both algae concentrations, algae reduced the Pb transfer rate from the

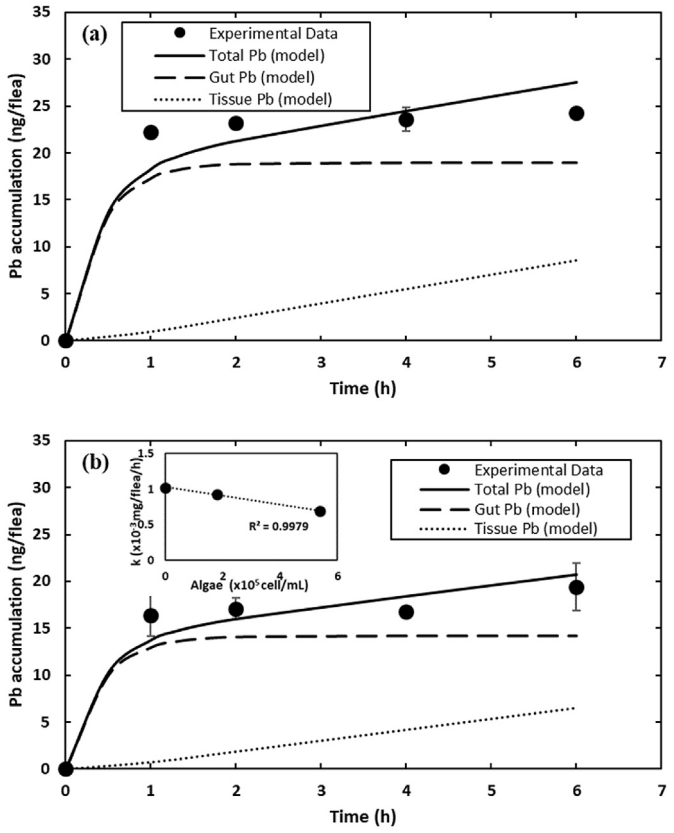

Fig. 4. The accumulation of Pb in *C. dubia* with different concentrations of algae. (a) 1.8×10^5 cell/mL of algae and (b) 5.4×10^5 cell/mL of algae. The small insert is the plot of Pb gut uptake constant as a function of algae concentration. Other conditions of the exposure medium: [Pb] = 2500 μg/L; [nano-TiO_2] = 50 mg/L.

gut to the tissue by approximately 50%, and also reduced the assimilation efficiency (AE) of Pb by approximately 50%. Because the ingestion of algae can reduce the gut passage time of nano-TiO_2 (Tan and Wang, 2017), the Pb transfer from the gut to the tissue and the Pb assimilation efficiency were reduced.

It is interesting to note that, for both algae concentrations, and even for a condition without algae, the gut depuration rate of constant k_{1e} was the same. The gut depuration of heavy metals is a physical-chemical process. The adsorbed Pb on nano-TiO_2 was first released as soluble Pb ions within the gut, and some of these ions were depurated from *C. dubia* through the anus. The desorption of Pb from nano-TiO_2 is controlled by the gut pH, which was relatively constant (pH = 6.0–6.8) under different conditions (Ebert, 2005). The algae might not change the gut pH and, thus, the gut depuration rate of constant k_{1e} was the same.

It is also important to note that, for both algae concentrations, the gut to tissue transfer rate of constant k_{12} was the same. Algae reduced the Pb transfer rate from the gut to the tissue due to dilution of the gut Pb by the algae. However, the Pb transfer from the gut to the tissue is a biological process, which depends on ion channels and protein transporters (Kiela and Ghishan, 2016). It is possible that different concentrations of algae did not change the biological activity that was related to the rate of Pb transfer from the gut to the tissue.

4.5. Effect of nano-TiO_2 on Pb toxicity

In a previous study we found that 2500 μg/L of Pb alone had very low accumulation and toxicity, with a 24 h mortality of less than 10%, but nano-TiO_2 significantly increased Pb toxicity (Liu et al., 2019). In addition, we found that nano-TiO_2 alone, up to 1000 mg/L, did not result the death of *C. dubia* (Hu et al., 2012a; Liu et al., 2019). Gillis et al. (2005) reported that a heavy metal accumulation in the tissue is responsible for toxicity. He et al. (2019) reported the positive relation between heavy metal body accumulation and toxicity. Together, these findings suggested that nano-TiO_2 enhanced Pb accumulation in tissue that develops toxicity. Fig. 5a shows that the observed survivorship of *C. dubia* decreased with an increase in exposure time (filled circles), which suggests that the decrease in survivorship correlates with the increase in Pb tissue accumulation.

Our previous research indicated that accumulations of heavy metals and NPs in adult *C. dubia* were positively correlated to toxicity in *C. dubia* neonates (Hu et al., 2012c; Liu et al., 2019; Wang et al., 2011a). Therefore, we can correlate the experimental survivorship data from *C. dubia* neonates (S(t)) with the projected Pb tissue accumulation in *C. dubia* adults during a 24 h exposure period ($C_{tissue}(t)$) by using the toxicodynamic model, Equation (8), to determine the relevant constants in the model. The estimated $C_{tissue}(t)$ during the 24 h accumulation period was calculated using Equation (11), based on parameters in Table 1, shown as the dotted curve in Fig. 5(a). The solid curve in Fig. 5(a) is the curve fitting results, which agrees with the experimental survivorship data. Based on the curve fitting, the Pb threshold concentration was determined to be C_{TH} = 25.87 ng/flea, and the killing rate was determined to be $k_k = 5 \times 10^{-4}$ flea/ng/h. These constants are also listed in Fig. 5(a). By comparing the survivorship data and the projected Pb tissue accumulation, it is apparent that the response of *C. dubia* to Pb toxicity was instantaneous, as soon as Pb tissue

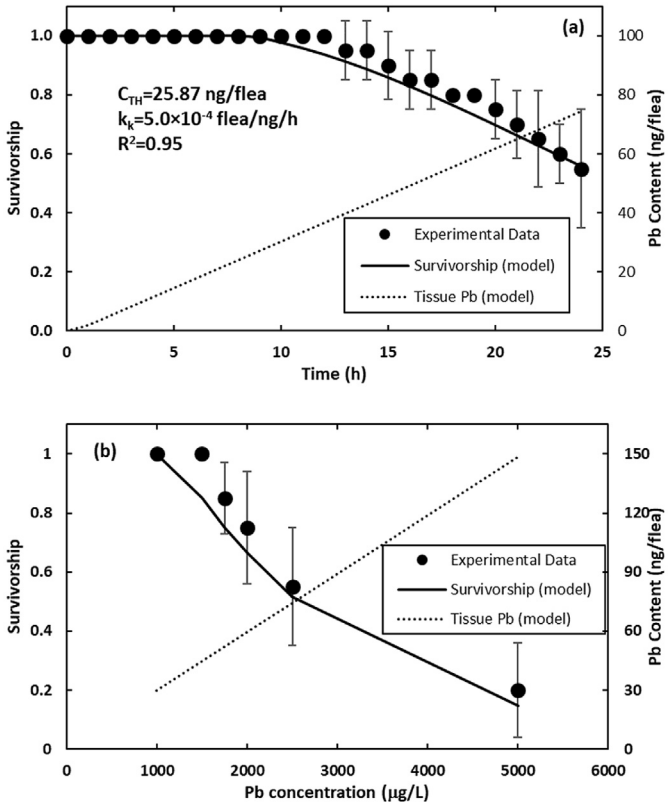

Fig. 5. Survival of *C. dubia* in the presence of Pb and nano-TiO_2. (a) Survival at different exposure times, using a test solution that contained 2500 μg/L of Pb and 50 mg/L of nano-TiO_2. (b) Survival for 24 h in test solutions that contain 50 mg/L of nano-TiO_2 and different concentrations of Pb (μg/L).

accumulation exceeds the threshold value. Therefore, the maximal Pb tissue accumulation at the end of the exposure period can be used to reflect the concentration factor during hazard assessment, as defined in Equation (8).

To validate the applicability of the two-compartment toxicodynamic model, Equations (8) and (11), we conducted independent 24 h toxicity experiments using a series of test solutions that contained 50 mg/L of nano-TiO_2 and different concentrations of Pb. Fig. 5(b) shows the experimental 24 h survivorship as a function of the Pb concentration data in filled circles.

The change in Pb concentration could proportionally alter the adsorption density of Pb on nano-TiO_2, thus changing the Pb accumulation in the gut due to its limited space for holding nano-TiO_2. This implies a change in Pb tissue accumulation and a consequential reduction of survivorship with increasing Pb concentration. To predict 24 h survivorship under different Pb concentrations, we first used the parameters developed in the Pb accumulation experiments in Table 1 to calculate Pb tissue accumulation using Equation (11), shown as the dotted line in Fig. 5(b). We then used the same Pb threshold concentration C_{TH} and the killing rate k_k determined through modeling the time-dependent survivorship data (Fig. 5(a)), and the toxicodynamic model Equation (8), to predict the 24 h survivorship of *C. dubia* under different Pb concentrations, shown as the solid curve in Fig. 5(b). The prediction results described the experimental data in the entire Pb concentration range very well. Consequently, the two-compartment toxicodynamic model, Equations (8) and (11), is appropriate to not only simulate Pb toxicity, but also predict Pb toxicity under other Pb concentrations, in the presence of 50 mg/L of nano-TiO_2. Note that Equation (11) can be combined with Equation (8) to directly calculate the survivorship of Pb as a function of Pb concentration and accumulation time, without actually calculating $C_{tissue}(t)$ as an intermittent step.

4.6. Algae impact on the combined toxicity of Pb and nano-TiO_2

Algae significantly reduced the combined toxicity of Pb and NPs. In this work, we quantified the algae effect on the combined toxicity of Pb and nano-TiO_2, using the two-compartment modeling approach. The time-dependent experimental survivorship data over a 24 h period, with 2500 μg/L of Pb, 50 mg/L of nano-TiO_2, and 1.8×10^5 cell/mL of algae, are shown in Fig. 6(a) (filled circles). To model these data using Equation (8), we first calculated the 24 h Pb tissue accumulation using Equation (11) and related constants in Table 1, shown as the dotted curve in Fig. 6(a). We then applied these values to Equation (8), to model the experimental survivorship data and determine the threshold concentration C_{TH} and the killing rate k_k for this particular test solution. The curve fitting results and the related model parameters are shown in Fig. 6(a).

The modeling results described the experimental survivorship data very well. Compared to Fig. 5(a), the presence of 1.8×10^5 cell/mL of algae significantly increased the survivorship of *C. dubia*. The parameters suggested that the ingestion of algae did not change the toxic metal threshold concentration C_{TH}, but reduced the killing rate k_k by approximately 15%. The major toxicity mechanism of heavy metals is the production of reactive oxygen species (ROS) (Ercal et al., 2001). Algae, as a food source, can provide energy to elevate antioxidant levels in organisms to neutralize ROS (Poljsak et al., 2013). In addition, some algae may directly serve as antioxidants (Kelman et al., 2012; Romay et al., 1998). Both of these effects could possibly mitigate the toxic effect of Pb and, thus, reduce the killing rate.

By comparing the parameters in the Pb accumulation modeling and the Pb toxicodynamic modeling, respectively, it was apparent that algae mitigated the combined toxicity of Pb and nano-TiO_2 through two aspects: physical and biological. In the physical aspect, algae spatially reduced Pb accumulation in the tissue of *C. dubia*. In the biological aspect, algae provided energy to organisms and reduced the killing rate.

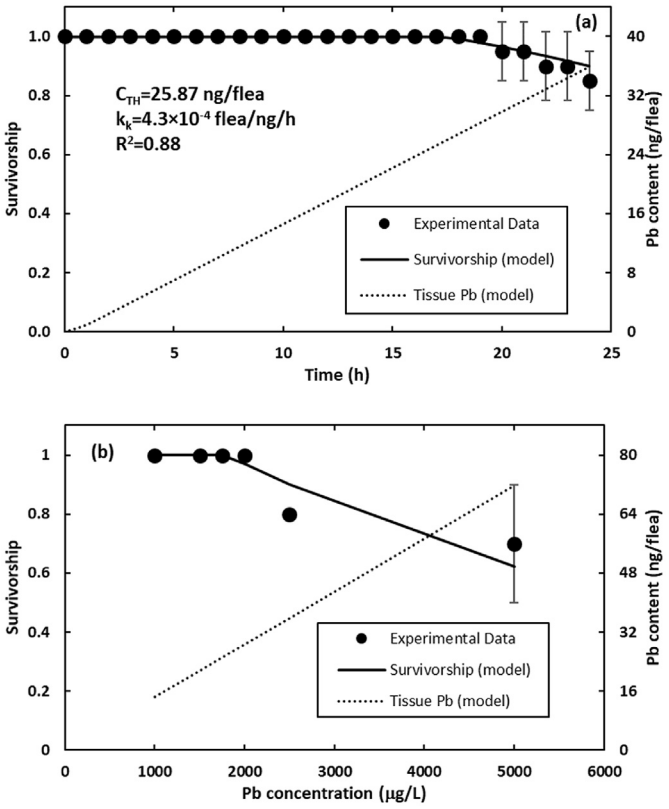

Fig. 6. Survival of *C. dubia* in the presence of Pb, nano-TiO_2, and algae. (a) The survival at different exposure times using a test solution that contained 2500 μg/L of Pb, 50 mg/L of nano-TiO_2, and 1.8×10^5 cell/mL of algae. (b) 24 h survival in test solutions that contained 50 mg/L of nano-TiO_2, 1.8×10^5 cell/mL of algae, and different concentrations of Pb (μg/L).

In order to validate the two-compartment toxicodynamic model in the presence of algae, we analyzed the 24 h toxicity test data obtained from test solutions that contained 50 mg/L of nano-TiO_2, 1.8×10^5 cell/mL of algae, and various concentrations of Pb. Fig. 6(b) shows the experimental data (filled circles) and the model prediction (solid curve). The model prediction was performed using Equations (8) and (11), based on parameters in Table 1 and Fig. 6(a). Fig. 6(b) shows that the model prediction was in agreement with the experimental data, indicating that the two-compartment modeling approach can be used to predict the combined toxicity of Pb and nano-TiO_2 in the presence of algae. Collectively, this two-compartment modeling approach provides a predictive tool for toxicity assessment under these complex conditions.

NPs could impact the toxicity of environmental toxins through multiple mechanisms, including adsorption/desorption, active uptake, diffusion, metabolic transfer, and many more. The presence of algae, a natural food source, makes this interaction more complex. Therefore, appropriate modeling is essential in integrating these impacts and providing a comprehensive understanding of toxicity mechanisms. This research links the two-compartment accumulation model that predicts the metal distribution within the *C. dubia*, with the toxicodynamic model that predicts the toxicity response of *C. dubia*. Consequently, advancement in interpreting the impacts of NPs in complex ecosystems can be achieved. This model could provide insight into the metal toxicity mechanisms in the presence of NPs from the perspective of metal accumulation. However, some

environmental conditions, such as NPs dissolution, presence of other toxic metals, organic matter, thermal stress, and pH, could lead the metal precipitation and/or speciation change, thereby altering toxicity behavior. The interactions among these conditions, the target heavy metal ion, and the organism responses need be considered when using this model to elucidate the toxicity mechanisms.

5. Conclusions

In this research we developed a two-compartment modeling approach to quantify Pb accumulation and toxicity in the presence of nano-TiO_2. The modeling results suggested that the Pb was quickly accumulated in the gut of *C. dubia*, and then slowly transferred to body tissue. The Pb toxicity was related to Pb accumulated in the body tissue and accumulation time, which can be quantified using this two-compartment modeling approach. Results also indicated that algae could reduce the combined toxicity of Pb and nano-TiO_2, and this effect could also be quantified using the two-compartment modeling approach. The model revealed that algae could reduce the Pb accumulation in *C. dubia* and the killing rate of Pb. However, 1.8×10^5 cell/mL of algae did not change the Pb tolerance level in *C. dubia*.

Credit author statement

Xuesong Liu: Conceptualization, Investigation, Writing - original draft, Writing - review & editing. Jianmin Wang: Supervision, Project administration, Writing - review & editing. Yue-Wern Huang: Supervision, Writing - review & editing.

Declaration of competing interest

The authors declare that they have no known competing financial interests or personal relationships that could have appeared to influence the work reported in this paper.

Acknowledgement

The authors greatly appreciate the support from the Center for Research in Energy and Environment (CREE) at Missouri S&T. The authors would also like to thank Natalie Holl from the Department of Biological Sciences for additional comments for this manuscript.

Appendix A. Supplementary data

Supplementary data to this article can be found online at https://doi.org/10.1016/j.chemosphere.2020.127958.

References

Ashauer, R., Hintermeister, A., Caravatti, I., Kretschmann, A., Escher, B.I., 2010. Toxicokinetic and toxicodynamic modeling explains carry-over toxicity from exposure to diazinon by slow organism recovery. Environ. Sci. Technol. 44 (10), 3963–3971.

Bundschuh, M., Filser, J., Lüderwald, S., McKee, M.S., Metreveli, G., Schaumann, G.E., Schulz, R., Wagner, S., 2018. Nanoparticles in the environment: where do we come from, where do we go to? Environ. Sci. Eur. 30 (1), 6-6.

Cedergreen, N., Dalhoff, K., Li, D., Gottardi, M., Kretschmann, A.C., 2017. Can toxicokinetic and toxicodynamic modeling be used to understand and predict synergistic interactions between chemicals? Environ. Sci. Technol. 51 (24), 14379–14389.

Ebert, D.P., 2005. Ecology, Epidemiology, and Evolution of Parasitism in Daphnia. National Library of Medicine (US), National Center for Biotechnology Information, Bethesda, MD.

EPA, 2002. Methods for Measuring the Acute Toxicity of Effluents and Receiving Waters to Freshwater and Marine Organisms.

Ercal, N., Gurer-Orhan, H., Aykin-Burns, N., 2001. Toxic metals and oxidative stress part I: mechanisms involved in metal-induced oxidative damage. Curr. Top. Med. Chem. 1 (6), 529–539.

Fan, W., Cui, M., Liu, H., Wang, C., Shi, Z., Tan, C., Yang, X., 2011. Nano-TiO_2 enhances the toxicity of copper in natural water to *Daphnia magna*. Environ. Pollut. 159 (3), 729–734.

Fan, W., Peng, R., Li, X., Ren, J., Liu, T., Wang, X., 2016. Effect of titanium dioxide nanoparticles on copper toxicity to *Daphnia magna* in water: role of organic matter. Water Res. 105, 129–137.

Gao, Y., Feng, J., Han, F., Zhu, L., 2016. Application of biotic ligand and toxicokinetic–toxicodynamic modeling to predict the accumulation and toxicity of metal mixtures to zebrafish larvae. Environ. Pollut. 213, 16–29.

Gillis, P.L., Chow-Fraser, P., Ranville, J.F., Ross, P.E., Wood, C.M., 2005. *Daphnia* need to be gut-cleared too: the effect of exposure to and ingestion of metal-contaminated sediment on the gut-clearance patterns of *D. magna*. Aquat. Toxicol. 71 (2), 143–154.

He, E., Qiu, H., Huang, X., Van Gestel, C.A.M., Qiu, R., 2019. Different dynamic accumulation and toxicity of ZnO nanoparticles and ionic Zn in the soil sentinel organism *Enchytraeus crypticus*. Environ. Pollut. 245, 510–518.

He, E., Qiu, R., Cao, X., Song, L., Peijnenburg, W.J.G.M., Qiu, H., 2020. Elucidating toxicodynamic differences at the molecular scale between ZnO nanoparticles and $ZnCl_2$ in *Enchytraeus crypticus* via nontargeted metabolomics. Environ. Sci. Technol. 54, 3487–3498.

Heinlaan, M., Ivask, A., Blinova, I., Dubourguier, H.C., Kahru, A., 2008. Toxicity of nanosized and bulk ZnO, CuO and TiO_2 to bacteria *Vibrio fischeri* and crustaceans *Daphnia magna* and *Thamnocephalus platyurus*. Chemosphere 71, 1308–1316.

Horton, P., Rowan, M., Webster, K., Peters, R., 1979. Browsing and grazing by cladoceran filter feeders. Can. J. Zool. 57 (1), 206–212.

Hu, J., Wang, D., Wang, J., Wang, J., 2012a. Toxicity of lead on *Ceriodaphnia dubia* in the presence of nano-CeO_2 and nano-TiO_2. Chemosphere 89 (5), 536–541.

Hu, J., Wang, D., Forthaus, B.E., Wang, J., 2012b. Quantifying the effect of nanoparticles on as (V) ecotoxicity exemplified by nano-Fe_2O_3 (magnetic) and nano-Al_2O_3. Environ. Toxicol. Chem. 31 (12), 2870–2876.

Hu, J., Wang, D., Wang, J., Wang, J., 2012c. Bioaccumulation of Fe_2O_3 (magnetic) nanoparticles in *Ceriodaphnia dubia*. Environ. Pollut. 162, 216–222.

ICMM, 2007. Health risk assessment guidance for metals. Fact Sheet 4.

Kelman, D., Posner, E.K., McDermid, K.J., Tabandera, N.K., Wright, P.R., Wright, A.D., 2012. Antioxidant activity of Hawaiian marine algae. Mar. Drugs 10, 403–416.

Kerper, L.E., Hinkle, P.M., 1997. Cellular uptake of lead is activated by depletion of intracellular calcium stores. J. Biol. Chem. 272 (13), 8346–8352.

Kiela, P.R., Ghishan, F.K., 2016. Physiology of intestinal absorption and secretion. Best Pract. Res. Clin. Gastroenterol. 30 (2), 145–159.

Lewis, J., 1985. Lead poisoning: a historical perspective. EPA J. 11, 15.

Liu, X., Wang, J., Huang, Y.-W., Kong, T., 2019. Algae (*Raphidocelis*) reduce combined toxicity of nano-TiO_2 and lead on *C. dubia*. Sci. Total Environ. 686, 246–253.

Pan, K., Tan, Q.-G., Wang, W.-X., 2016. Two-compartment kinetic modeling of radiocesium accumulation in marine bivalves under hypothetical exposure regimes. Environ. Sci. Technol. 50 (5), 2677–2684.

Petersen, E.J., Akkanen, J., Kukkonen, J.V., Weber Jr., W.J., 2009. Biological uptake and depuration of carbon nanotubes by *Daphnia magna*. Environ. Sci. Technol. 43 (8), 2969–2975.

Poljsak, B., Suput, D., Milisav, I., 2013. Achieving the balance between ROS and antioxidants: when to use the synthetic antioxidants. Oxid. Med. Cell. Longev. 2013, 956792.

Romay, C., Armesto, J., Remirez, D., Gonzalez, R., Ledon, N., Garcia, I., 1998. Antioxidant and anti-inflammatory properties of C-phycocyanin from blue-green algae. Inflamm. Res. 47, 36–41.

Silver, S., 1996. Bacterial resistances to toxic metal ions-a review. Gene 179 (1), 9–19.

Su, Y., Tong, X., Huang, C., Chen, J., Liu, S., Gao, S., Mao, L., Xing, B., 2018. Green algae as carriers enhance the bioavailability of 14C-labeled few-layer graphene to freshwater snails. Environ. Sci. Technol. 52 (3), 1591–1601.

Svensson, S., 2003. Depuration of okadaic acid (Diarrhetic Shellfish Toxin) in mussels, *Mytilus edulis* (Linnaeus), feeding on different quantities of nontoxic algae. Aquaculture 218 (1–4), 277–291.

Tan, C., Fan, W.-H., Wang, W.-X., 2011. Role of titanium dioxide nanoparticles in the elevated uptake and retention of cadmium and zinc in *Daphnia magna*. Environ. Sci. Technol. 46 (1), 469–476.

Tan, C., Wang, W.-X., 2017. Influences of TiO_2 nanoparticles on dietary metal uptake *in Daphnia magna*. Environ. Pollut. 231, 311–318.

Tan, L.-Y., Huang, B., Xu, S., Wei, Z.-B., Yang, L.-Y., Miao, A.-J., 2016. TiO_2 nanoparticle uptake by the water flea *Daphnia magna* via different routes is calcium-dependent. Environ. Sci. Technol. 50 (14), 7799–7807.

Tan, Q.-G., Wang, W.-X., 2012. Two-compartment toxicokinetic–toxicodynamic model to predict metal toxicity in *Daphnia magna*. Environ. Sci. Technol. 46 (17), 9709–9715.

Wang, D., Hu, J., Forthaus, B.E., Wang, J., 2011a. Synergistic toxic effect of nano-Al_2O_3 and As(V) on *Ceriodaphnia dubia*. Environ. Pollut. 159 (10), 3003–3008.

Wang, D., Hu, J., Irons, D.R., Wang, J., 2011b. Synergistic toxic effect of nano-TiO_2 and As(V) on *Ceriodaphnia dubia*. Sci. Total Environ. 409 (7), 1351–1356.

Wang, J., Pantopoulos, K., 2011. Regulation of cellular iron metabolism. Biochem. J. 434 (3), 365–381.

Wang, Z., Luo, Z., Yan, C., Che, F., Yan, Y., 2014. Arsenic uptake and depuration kinetics in *Microcystis aeruginosa* under different phosphate regimes. J. Hazard Mater. 276, 393–399.

WolframAlpha, 2009. https://www.wolframalpha.com/examples/mathematics/differential-equations/. (Accessed 31 March 2020).